# Kinetic Studies on the Oxidation of η 5 Cyclopentadienyl Methyl Tricarbonyl Molybdenum(II) and the Use of Its Oxidation Products as Olefin Epoxidation Catalysts

**ARTICLE** *in* ORGANOMETALLICS · JANUARY 2009

Impact Factor: 4.13 · DOI: 10.1021/om8009206

ORGANOMETALLICS



Article

# Kinetic Studies on the Oxidation of #-Cyclopentadienyl Methyl Tricarbonyl Molybdenum(II) and the Use of Its Oxidation Products as Olefin Epoxidation Catalysts

Ahmad M. Al-Ajlouni, Draganco Veljanovski, Alejandro Capape#, Jin Zhao, Eberhardt Herdtweck, Maria Jose# Calhorda, and Fritz E. Ku#hn

*Organometallics*, **2009**, 28 (2), 639-645• DOI: 10.1021/om8009206 • Publication Date (Web): 29 December 2008



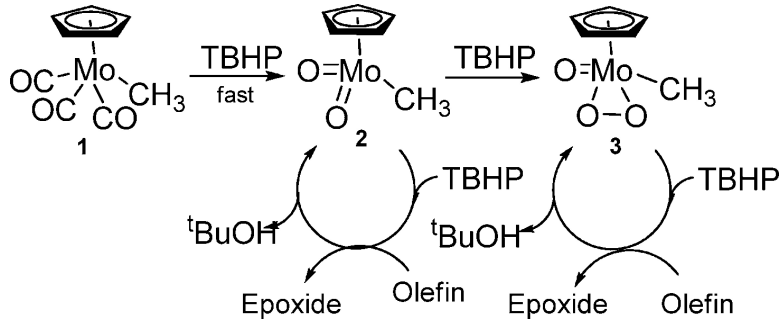


## More About This Article

Additional resources and features associated with this article are available within the HTML version:

- Supporting Information
- Access to high resolution figures
- Links to articles and content related to this article
- Copyright permission to reproduce figures and/or text from this article

View the Full Text HTML



Organometallics is published by the American Chemical Society. 1155 Sixteenth Street N.W., Washington, DC 20036

# Kinetic Studies on the Oxidation of $\eta^5$-Cyclopentadienyl Methyl Tricarbonyl Molybdenum(II) and the Use of Its Oxidation Products as Olefin Epoxidation Catalysts

Ahmad M. Al-Ajlouni,[†,‡] Draganco Veljanovski,[†] Alejandro Capapé,[†] Jin Zhao,[†,§] Eberhardt Herdtweck,[†] Maria José Calhorda,[⊥] and Fritz E. Kühn*[,†]

*Molecular Catalysis, Faculty of Chemistry, Technische Universität München, Lichtenbergstrasse 4, D-85747 Garching bei München, Germany, Department of Applied Chemical Sciences, Jordan University of Science and Technology, Irbid 22110, Jordan, Department of Chemistry, National University of Singapore, 3 Science Drive 3, Kent Ridge, 117543, Singapore, and Departamento de Química e Bioquímica, CQB, Faculdade de Ciências, Universidade de Lisboa, 1749-016 Lisboa, Portugal*

*Received September 22, 2008*

The oxidation of $\eta^5$-cyclopentadienyl(methyl)(tricarbonyl)molybdenum(II) (**1**) with excess *tert*-butylhydroperoxide (TBHP) initially yields $\eta^5$-cyclopentadienyl(methyl)(dioxo)molybdenum(VI) (**2**), which further reacts with TBHP, forming $\eta^5$-cyclopentadienyl(methyl)(oxo)(peroxo)molybdenum(VI) (**3**). The solid-state structure of **3** has been determined by single-crystal X-ray crystallography. Detailed kinetic studies have been carried out on the oxidation of **1** with TBHP as an oxidizing agent and on the catalytic activities of the resulting oxidation products, **2** and **3**, in olefin epoxidation. In the absence of oxidant, neither of the molybdenum species is able to transfer an O-atom to an olefin. However, both Mo(VI) species act as catalysts for the epoxidation of olefins with TBHP through the formation of active intermediates. It has been found that compound **3** reacts with excess TBHP to give an active intermediate, which exists in equilibrium with the catalyst precursor **3** with a $K_{eq}$ close to 1. This intermediate is slowly formed in a reversible initial step. It reacts rapidly with an olefin, while it decomposes in the absence of olefin. Furthermore, the kinetic results indicate the formation of another active intermediate, originating from **2**, that is 3−5 times more active in epoxidation catalysis than the active intermediate formed from **3**. A mechanistic scheme is proposed, based on the kinetic results.

## 1. Introduction

Propylene oxide is an important intermediate in chemical industry, with an annual production of several million tons.[1] Propylene oxide is particularly important in the large-scale synthesis of propylene glycol, polyurethanes, and resins. A method that has been applied for a long time for the synthesis of propylene oxide is the chlorhydrine route. This method, however, consumes a considerable amount of $Cl_2$ and has a negative environmental impact. For the last decades significant research efforts both in industry and at universities have been dedicated to finding more efficient and environmentally benign synthetic pathways to propylene oxide and other valuable epoxides.[2] ARCO and Halcon described a catalytic process for the synthesis of epoxides in the late 1960s,[3] and since then many research groups concentrated on mechanistic aspects of these catalytic reactions and on finding improved catalysts.[4−6]

Among the variety of efficient catalysts known today for olefin epoxidation are some organometallic oxides containing a metal in high oxidation state.[7] Some of them can be conveniently synthesized from carbonyl precursors, such as $Cp'Mo(CO)_3R$ (R = alkyl group).[8−11] It has been found that

* Corresponding author. E-mail: fritz.kuehn@ch.tum.de.
† Technische Universität München.
‡ Jordan University of Science and Technology.
§ National University of Singapore.
⊥ Universidade de Lisboa.

(1) (b) Weissermel K., Arpe H. J. *Industrial Organic Cemistry*; Wiley: New York, 2003.

(2) (a) Bäckvall, J. E., Ed. *Modern Oxidation Methods*; Wiley-VCH: Weinheim, 2004. (b) Yudin, A. K., Ed. *Aziridines and Epoxides in Organic Synthesis*; Wiley-VCH: Weinheim, 2006.

(3) (a) Kollar J. (Halcon) US 3.350.422, US 3.351.635, 1967. (b) Sheng M. N., Zajaczek G. J. (ARCO) GB 1.136.923, 1968. (c) Coltan, R.; Tomkins, I. B. *Aust. J. Chem.* **1965**, *18*, 447.

(4) (a) Fischer, E. O.; Vigoureux, S. *Chem. Ber.* **1958**, *91*, 1342. (b) Fischer, E. O.; Ulm, K.; Fritz, H. P. *Chem. Ber.* **1960**, *93*, 2167. (c) Cousins, M.; Green, M. L. H. *J. Chem. Soc.* **1963**, 889. (d) Nunes, C. D.; Valente, A. A.; Pillinger, M.; Rocha, J.; Gonçalves, I. S. *Chem.−Eur. J.* **2003**, *9*, 4380. (e) Abrantes, M.; Valente, A. A.; Pillinger, M.; Gonçalves, I. S.; Rocha, J.; Romão, C. C. *Inorg. Chem. Commun.* **2002**, *5*, 1069. (f) Abrantes, M.; Valente, A. A.; Pillinger, M.; Gonçalves, I. S.; Rocha, J.; Romão, C. C. *J. Catal.* **2002**, *209*, 237.

(5) (a) Herrmann, W. A.; Kühn, F. E. *Acc. Chem. Res.* **1997**, *30*, 169. (b) Deubel, D. V.; Frenking, G.; Gisdaks, P.; Herrmann, W. A.; Rösch, N.; Sundermeyer, J. *Acc. Chem. Res.* **2004**, *37*, 645. (c) Chong, A. O.; Sharpless, K. B. *J. Org. Chem.* **1977**, *42*, 1587. (d) Sheng, M. N.; Zajacek, J. G. *J. Org. Chem.* **1970**, *35*, 1839. (e) Sheldon, R. A.; van Doorn, J. A. *J. Catal.* **1973**, *31*, 427. (f) Sheldon, R. A.; van Doorn, J. A. A.; Schram, C. W. A.; de Jong, J. *J. Catal.* **1973**, *31*, 438.

(6) (a) Sheldon, R. A. *Recl. Trav. Chim.* **1973**, *92*, 253. (b) Thiel, W. R. *J. Mol. Catal. A: Chem.* **1997**, *117*, 449. (c) Wahl, G.; Kleinhenz, D.; Schorm, A.; Sundermeyer, J.; Stowasser, R.; Rummey, C.; Bringmann, G. *Chem.−Eur. J.* **1999**, *5*, 3237. (d) Poli, R. *Chem.−Eur. J.* **2004**, *10*, 332. (e) Chaumette, P.; Mimoun, H.; Saussine, L. *J. Organomet. Chem.* **1983**, *250*, 291. (f) Trost, M. K.; Bergman, R. G. *Organometallics* **1991**, *10*, 1172.

(7) (a) Kühn, F. E.; Santos, A. M.; Abrantes, M. *Chem. Rev.* **2006**, *106*, 2455. (b) Romão, C. C.; Kühn, F. E.; Herrmann, W. A. *Chem. Rev.* **1997**, *97*, 3197.

(8) (a) Faller, J. W.; Ma, Y. *J. Organomet. Chem.* **1988**, *340*, 59. (b) Faller, J. W.; Ma, Y. *J. Organomet. Chem.* **1989**, *368*, 45. (c) Bottomley, F.; Boyle, P.; Chen, J. *Organometallics* **1994**, *13*, 370.

(9) (a) Zhao, J.; Santos, A. M.; Herdtwerk, E.; Kühn, F. E. *J. Mol. Catal. A: Chem.* **2004**, *222*, 265. (b) Radius, U.; Wahl, G.; Sundermeyer, J. *Z. Anorg. Allg. Chem.* **2004**, *630*, 848. (c) Robin, T.; Montilla, F.; Galindo, A.; Ruiz, C.; Hartmann, J. *Polyhedron* **1999**, *18*, 1485. (d) Pratt, M.; Harper, J. H. M.; Colbran, S. B. *Dalton Trans.* **2007**, 2746.

10.1021/om8009206 CCC: $40.75 
Publication on Web 12/29/2008

the latter catalyze the epoxidation of olefins with *tert*-butyl hydroperoxide (TBHP) and other alkyl hydroperoxides as oxidants.[8,9]

The most thoroughly examined organometallic epoxidation catalyst known today is arguably methyltrioxorhenium, $CH_3ReO_3$. In this particular case peroxo derivatives have been shown to be the active catalysts, and metal-attached $\eta^2$-peroxo groups react with olefins when applied stoichiometrically.[12−14] Compounds of formula $Cp'Mo(CO)_3R$ and their oxidation products[15] have not yet been examined in comparable detail, particularly with respect to mechanistic implications, and no active species beyond the Mo(VI)-dioxo species has been found or proposed to date. However, catalytic results show that their catalytic activity is considerable, and, in contrast to MTO they are both easier to derivatize and easier to immobilize.[7−11,16] In this work, a detailed examination of the reaction mechanism of $Cp'Mo(CO)_3R$-based olefin epoxidation with TBHP as the oxidizing agent is presented, based on kinetic experiments. It involves a comprehensive investigation of the system starting with (1) the tricarbonyl, (2) the dioxo, and (3) the oxo peroxo compounds after adding excess TBHP in the presence and absence of olefin. Detailed kinetic studies have also been carried out on the activity of an oxo peroxo-derived active species with respect to olefin epoxidation with TBHP.

## 2. Results and Discussion

The title compound, $CpMo(CO)_3CH_3$ (**1**), was synthesized and purified using a slightly modified literature method.[17] When the carbonyl compound is treated with a TBHP excess of at least 5 equiv in dichloromethane, the Mo(VI)oxo-peroxo complex **3** is formed and can be isolated in good yields.

Compound **3** was characterized by UV−vis, IR, and NMR spectroscopy (see Experimental Section), and the structure was determined by single-crystal X-ray diffraction (see Supporting Information).

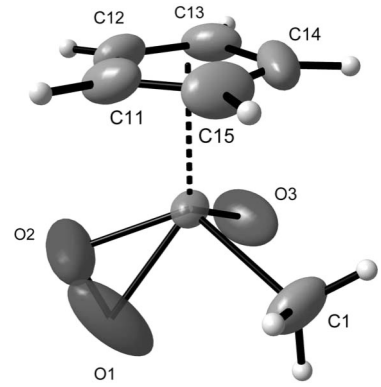


**Figure 1.** ORTEP-style plot of compound **3** in the solid state. Thermal ellipsoids are drawn at the 50% probability level. Details of the single-crystal X-ray diffraction studies are given in the Supporting Information.

**Scheme 1. Synthesis of Mo(VI)oxo-peroxo Compound 3**

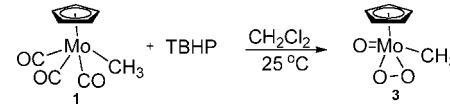


The single-crystal X-ray crystallographic analysis of compound **3** reveals that its solid-state molecular structure displays a slightly distorted "three-legged piano stool" conformation, in which the midpoint of the peroxo ligand is one of the legs of the piano stool. Two other structurally characterized Mo oxo-peroxo compounds and three W(VI)-oxoperoxo compounds of composition $Cp'WO(O_2)(CH_2SiMe_3)$ and $Cp^*WO(O_2)Cl$ have a similar structural arrangement according to the literature.[15a,18]

**Kinetic Studies. Reaction of $CpMo(CO)_3CH_3$ (1) with TBHP.** The reaction of **1** with TBHP was carried out at room temperature and followed by NMR (in dry $CDCl_3$) and UV−vis (in dry $CH_2Cl_2$) spectroscopic techniques, respectively. The changes in the chemical shifts of the Cp and/or the methyl protons in the NMR spectra are particularly informative. When 0.06 mmol of **1** and 10 equiv of TBHP are mixed in 0.5 mL of $CDCl_3$, the reaction starts immediately. The Cp signal of the carbonyl compound at 5.27 ppm decreases with time, and a new signal at 6.33 ppm appears. The area of this new signal reaches a maximum after 15 min, whereas the carbonyl compound peak is reduced to around 60% of its original size. The reduction of the signal at 6.33 ppm is associated with the buildup of a new signal at 6.29 ppm. After 2 h, the Cp signal of the carbonyl compound and the Cp signal at 6.33 ppm disappear completely, and only the signal at 6.29 ppm remains. The signal intensity−time curves are shown in Figure 2A. The $^{95}$Mo NMR examination shows similar results. After 2 h the $^{95}$Mo signal of **1** at −1424 ppm vanishes completely, and a new peak at −609 ppm, which has been assigned to the complex **3** is the only one observed.[7a] An intermediate forming and disappearing in the same time frame as for the $^1$H NMR experiments is observed at −346 ppm.

An experiment was designed to examine the compound (at 6.33 ppm), which is usually formed shortly after mixing TBHP with the carbonyl compound and later disappears. The above reaction was repeated and quenched after 15 min by adding $MnO_2$. The filtrate is evaporated to dryness and extracted with diethyl ether to give a yellow solid. The product is analyzed by

(10) Zhao, J.; Sakthivel, A.; Santos, A. M.; Kühn, F. E. *Inorg. Chim. Acta* **2005**, *358*, 4201.

(11) Honzicek, J.; Almeida Paz, F. A.; Romão, C. C. *Eur. J. Inorg. Chem.* **2007**, 2827.

(12) (a) Hroch, A.; Thiel, W. R.; Gemmecker, G. *Eur. J. Inorg. Chem.* **2000**, 1107, and references therein. (b) Kühn, F. E.; Groarke, M.; Bencze, É.; Herdtweck, E.; Prazeres, A.; Santos, A. M.; Calhorda, M. J.; Romão, C. C.; Gonçalves, I. S.; Lopes, A. D.; Pillinger, M. *Chem.−Eur. J.* **2002**, *8*, 2370–2383. (c) Veiros, L. F.; Prazeres, A.; Costa, P. J.; Romão, C. C.; Kühn, F. E.; Calhorda, M. J. *Dalton Trans.* **2006**, 1383. (d) Al-Ajlouni, A. M.; Valente, A. A.; Nunes, C. D.; Pillinger, M.; Santos, T. M.; Zhao, J.; Romão, C. C.; Gonçalves, I. S.; Kühn, F. E. *Eur. J. Inorg. Chem.* **2005**, 1716. (e) Al-Ajlouni, A.; Espenson, J. H. *J. Am. Chem. Soc.* **1995**, *117*, 9243. (f) Al-Ajlouni, A.; Espenson, J. H. *J. Org. Chem.* **1996**, *61*, 3969. (g) Espenson, J. H. *J. Chem, Soc., Chem. Commun.* **1999**, 479.

(13) (a) Herrmann, W. A.; Fischer, R. W.; Scherer, W.; Rauch, M. U. *Angew. Chem., Int. Ed.* **1993**, *32*, 1157. (b) Herrmann, W. A.; Fischer, R. W.; Rauch, M. U.; Scherer, W. *J. Mol. Catal.* **1994**, *86*, 243.

(14) (c) Kühn, F. E.; Santos, A. M.; Roesky, P. W.; Herdtweck, E.; Scherer, W.; Gisdakis, P.; Yudanov, I. V.; Di Valentin, C.; Rösch, N. *Chem.−Eur. J.* **1999**, *5*, 3603.

(15) (a) Legzdins, P.; Phillips, E. C.; Rettig, S. J.; Sánchez, L.; Trotter, J.; Yee, V. C. *Organometallics* **1988**, *7*, 1877. (b) Legzdins, P.; Phillips, E. C.; Sánchez, L. *Organometallics* **1989**, *8*, 940.

(16) (a) Zhao, J.; Herdtwerk, E.; Kühn, F. E. *J. Organomet. Chem.* **2006**, *691*, 2199. (b) Zhao, J.; Jain, K. R.; Herdtweck, E.; Kühn, F. E. *Dalton. Trans.* **2007**, 5567.

(17) (a) Burgmayer, S. J. N.; Templeton, J. L. *Inorg. Chem.* **1985**, *24*, 2224. (b) Abrantes, M.; Gago, S.; Valente, A. A.; Pillinger, M.; Gonçalves, I. S.; Santos, T. M.; Rocha, J.; Romão, C. C. *Eur. J. Inorg. Chem.* **2004**, 4914. (c) King, R. B.; Bisnette, M. B. *J. Organomet. Chem.* **1967**, *8*, 287. (d) Herrmann, W. A. In *Synthetic Methods of Organometallic and Inorganic Chemistry*; Herrmann, W. A., Ed. Georg Thieme Verlag: New York, 1997; Vol. 8, p 97. (e) Herrmann, W. A. In *Synthetic Methods of Organometallic and Inorganic Chemistry*; Herrmann, W. A.; Ed. Georg Thieme Verlag: New York, 1997; Vol *8*, p 98.

(18) (a) Faller, J. W.; Ma, Y. *Organometallics* **1988**, *7*, 559. (b) Trost, M. K.; Green, M. L. H. *Organometallics* **1991**, *10*, 1172. (c) Chakraborty, D.; Bhattacharjee, H.; Krätzner, R.; Siefken, Roesky, H. W.; Usón, I.; Schmidt, H. G. *Organometallics* **1999**, *18*, 106.

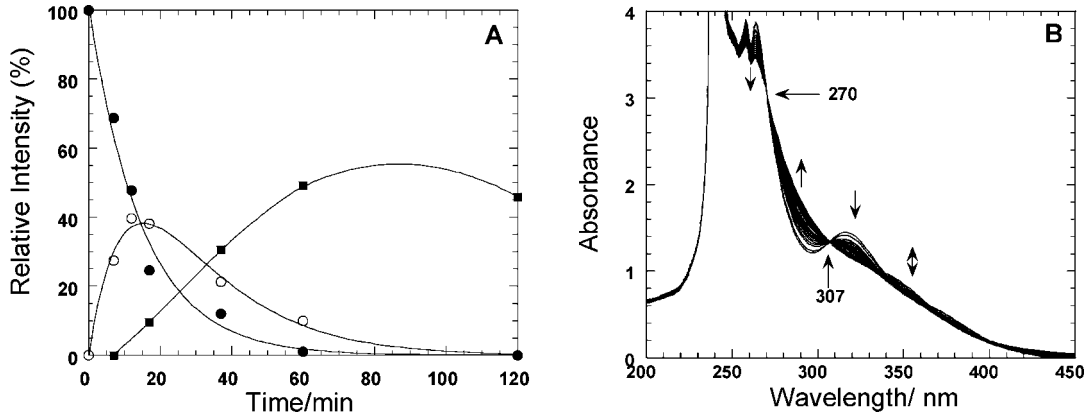


**Figure 2.** (A) Changes in the relative peak intensities with time of **1** (●) (at $\delta = 5.27$ ppm) and its products **2** (○) (at $\delta = 6.33$ ppm) and **3** (■) (at $\delta = 6.29$ ppm) during the reaction of **1** (0.06 mmol) with 10 equiv of TBHP in $CDCl_3$ at 20 °C. (B) UV−vis spectral changes (at 6 min intervals for the first 1 h and then every 10 min) for the reaction of **1** (0.33 mM) with TBHP (10 equiv) in $CH_2Cl_2$ at 20 °C.

**Scheme 2. Proposed Reaction Pathway for the Oxidation of Compound 1**

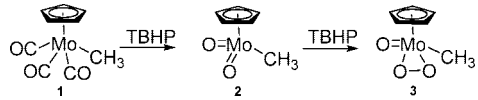


$^1$H and $^{95}$Mo NMR spectroscopy. The $^1$H NMR spectrum shows a signal at 6.33 ppm and a signal at 1.45 ppm with 5:3 relative intensities, respectively. The $^{95}$Mo NMR shows one signal at −346 ppm. A similar reaction profile can be obtained if the reaction is carried out in $C_6D_6$ under the same conditions, and the chemical shifts match with the NMR data for the dioxo-Mo(VI) compound, $CpMoO_2CH_3$ (**2**).[15b] These results suggest that the formation of **3** from the reaction of the carbonyl compound **1** with TBHP proceeds via compound **2**, as shown in Scheme 2.

The yield of the final product, compound **3**, in the NMR experiments described above is less than 60% (with respect to **1**), due to a side reaction, which forms a highly insoluble precipitate. The latter was isolated as a blue solid, containing 42.3% of Mo, 18.7% of C, and 2.9% of H. Further characterization attempts were unsuccessful due to its insolubility in all common solvents. The blue solid can also not be redissolved by adding excess TBHP. It has been further tested as a catalyst in olefin epoxidation and was found to be completely inactive, even after prolonged reaction times.

The yield of compound **3** can be increased by increasing the TBHP/**1** ratio, suggesting that the major reaction pathway, which leads to the relatively stable product **3**, is favored. The side reaction pathway is totally suppressed with the addition of a substrate in the catalytic reaction.

The reaction progress was also followed by UV−vis spectroscopy with different concentrations and catalyst/TBHP ratios in $CH_2Cl_2$. One has strong absorptions at $\lambda_{max} = 256$, 267, and 316 nm and a shoulder peak at $\lambda_{max} \sim 370$ nm. When the carbonyl complex (0.33 mM) is treated with a 10-fold excess of TBHP at room temperature, the absorbance at 316 nm decreases with time and the absorbance in the range 207−270 nm increases to give two clear isosbestic points at 307 and 270 nm (Figure 2B). These changes in absorbance are due to the formation of complex **2**. The reaction of **2** with TBHP proceeds, leading to an additional absorbance decrease in the range 307−335 nm and a slight increase in the absorbance in the range 335−400 nm, due to the formation of compound **3**. However, the isosbestic points due to this change are not all entirely clear; a possible explanation, based on further experimental evidence, is given in the next section. It is worth mentioning, however, that under UV experimental conditions no precipitate was observed, possibly due to the higher TBHP excess that may decrease catalyst decomposition or side reactions.

The intensity−time curves and the changes in the UV absorbance with time can be used to determine the rate constants for the oxidation of the carbonyl compound **1** with TBHP to yield **2** and the formation of **3** from compound **2**. In the presence of excess TBHP, the reactions follow pseudo-first-order kinetics, and the decrease in the intensity of the signal at 5.27 ppm (Cp protons of the carbonyl compound) with time fits a first-order exponential decay equation ($I_t = I_\infty + (I_o - I_\infty) \exp(-k_\Psi t)$). The value of the observed first-order rate constant was obtained from this fitting as $k_\Psi = (1.12 \pm 0.15) \times 10^{-3}$ s$^{-1}$. This indicates that the reaction is first-order with respect to the concentration of **1**. The buildup and the decay of the signal intensity at 6.33 ppm (Cp protons of **2**) was fitted to a biexponential (buildup and decay) equation to determine the pseudo-first-order constants for the formation of **2** ($k_f = (1.25 \pm 0.35) \times 10^{-3}$ s$^{-1}$) and for its reaction with TBHP ($k_r = (8.5 \pm 0.3) \times 10^{-4}$ s$^{-1}$). The rate constant $k_f$ is also valid for the reaction of the carbonyl compound with TBHP and is in accord with the value obtained above from the time-dependent decrease of the carbonyl signal. These kinetic results confirm the observations made when **2** is prepared from **1** in the presence of excess TBHP. The oxoperoxo compound **3** starts appearing immediately after **2** is formed because the two rate constants for the formation of **2** and its reaction with TBHP to produce **3** are comparable.

Previous studies on $CpMo(CO)_3Cl$-type compounds indicate that the Mo-dioxo moiety is rapidly formed in the case of the Cl-containing compounds but reacts more slowly with additional TBHP to yield the final Mo-oxoperoxo product.[18,15] From the results obtained here, it appears that the presence of a methyl group instead of a chloro ligand does not strongly affect the initial oxidation rate from Mo(II) to Mo(VI). However, the presence of a methyl group seems to enhance significantly the displacement rate of the oxo with the peroxo group on the Mo(VI) center. This difference in behavior of the Mo(VI) species between the Cl and the $CH_3$ derivative seems to become more pronounced in the further reaction between compound **3** and TBHP, where compound **3** can be transformed to an active species (**I**, see below), while the Cl derivative has been reported not to form an active catalyst in the presence of TBHP.[18]

**Reaction of $CpMoO(O)_2CH_3$ (3) with TBHP.** When **3** reacts with a large excess of TBHP (>100 equiv) in the absence of an olefin, a slight change of its UV−vis spectra occurs. After

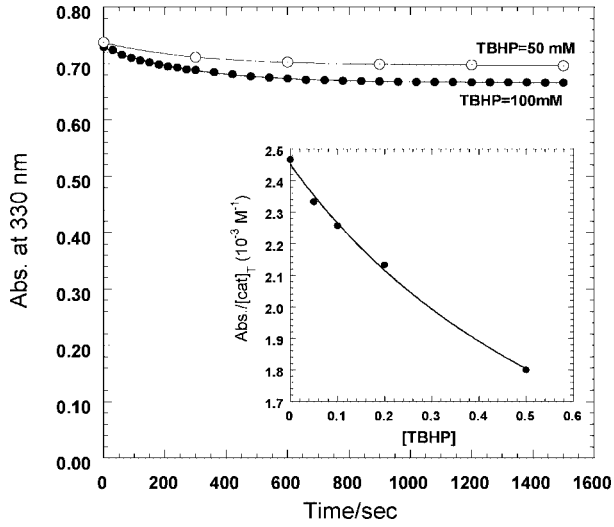


**Figure 3.** Changes in absorbance with time at 330 nm for the reaction of **3** with TBHP in $CH_2Cl_2$ at 20 °C. The inset shows a plot of $Abs_{eq}/[Mo]_T$ against [TBHP]; the solid line represents the calculated values based on eq 1 with $K_{eq} = 1.23$, $\varepsilon_I = 748$ $M^{-1}$ $cm^{-1}$, and $\varepsilon_p = 2460$ $M^{-1}$ $cm^{-1}$.

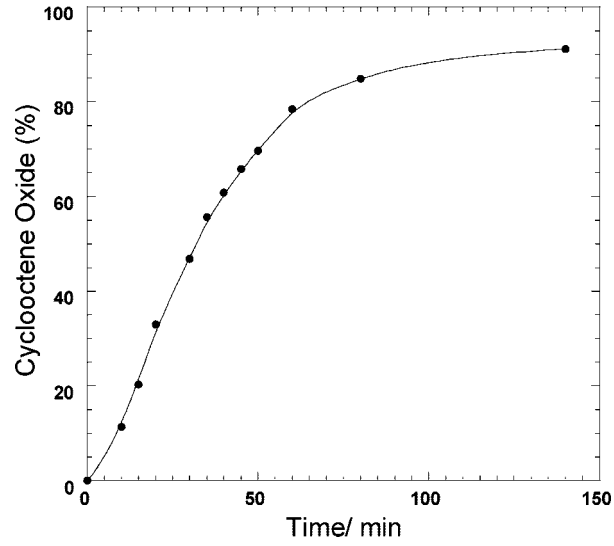


**Figure 4.** Yield of cyclooctene oxide against time. The reaction was carried out using 0.44 mmol of cyclooctene, 0.6 mmol of TBHP, and 0.05 mmol of **1** in $CDCl_3$ at 20 °C.

mixing a 0.3 mM solution of **3** in $CH_2Cl_2$ (total volume 3 mL) with 0.15 mmol of TBHP at room temperature, the absorbance at 330 nm decreases exponentially with time and levels off after ~20 min. By adding more TBHP, the absorbance decreases further but never becomes zero even with very high TBHP excess (~1500 equiv), as shown in Figure 3. This must be due to the formation of an intermediate (**I**), which exists in equilibrium with **3**.

$$\mathbf{3} + \mathrm{TBHP} \overset{K_{eq}}{\rightleftharpoons} \mathbf{I}$$

The equilibrium constant and the extinction coefficient of the intermediate were determined from the variation of the equilibrium absorbance with [TBHP] using eq 1. This equation is derived from the equilibrium expression and the mass-balance equation ($[Mo]_T = [\mathbf{3}] + [\mathbf{I}]$). Complete derivation of eq 1 is shown in Appendix I (Supporting Information),

$$\frac{Abs_{eq}}{[Mo]_T} = \varepsilon_I + \frac{(\varepsilon_p - \varepsilon_I)}{1 + K_{eq}[TBHP]} \quad (1)$$

where $Abs_{eq}$ is the absorbance at equilibrium, $[Mo]_T$ is the initial concentration of **3**, $\varepsilon_I$ and $\varepsilon_p$ are the extinction coefficients of the intermediate and **3**, respectively.

A plot of $Abs_{eq}/[Mo]_T$ against [TBHP] is shown as an inset in Figure 3. The data were fitted to eq 1, and the values of $K_{eq}$ ($= 1.23 \pm 0.49$) and $\varepsilon_I$ ($= 748 \pm 430$ $M^{-1}$ $cm^{-1}$ at 330 nm) were determined.

The absorbance−time curves in Figure 3 are exponential and fit to a first-order exponential equation, $A_t = A_\infty + (A_o - A_\infty)\exp(-k_\Psi t)$, to determine the values of $k_\Psi$ at each [TBHP]. The observed first-order rate constants ($k_\Psi$) vary linearly with [TBHP] in a relatively large intercept (Figure S3). Since the reaction between TBHP and **3** is reversible, the observed rate constant is the sum of the forward and the reverse rate constant. With TBHP being present in large excess over the catalyst, the observed rate constant can be expressed as

$$k_\Psi = k_p[TBHP] + k_{-p} \quad (2)$$

Therefore, the intercept of the straight line represents the value of the reverse rate constant ($k_{-p} = 0.0032 \pm 0.0002$ $s^{-1}$), and the slope expresses the forward rate constant ($k_p = 0.0047 \pm 0.0003$ $M^{-1}$ $s^{-1}$). The value of the equilibrium constant ($K_{eq} = 1.47 \pm 0.36$) calculated from these kinetic data agrees with the value ($K_{eq} = 1.23$) obtained from eq 1 within the experimental error range of these measurements. After the equilibrium is established, a slow decrease in the absorbance continues with time, probably due to the decomposition of the catalytic system, in the absence of olefin and increases with the TBHP concentration and the solvent polarity.[10]

**Catalytic Epoxidation. Epoxidations Starting from $CpMo(CO)_3CH_3$ (1).** Since the olefin does not react with TBHP without the catalyst being present, no corrections were needed for the uncatalyzed process. In the presence of an olefin, the epoxide is formed and the conversion to the epoxide proceeds to completion. Figure 4 shows the formation of cyclooctene oxide with time in an NMR experiment initially started with **1** (0.05 mmol), TBHP (0.6 mmol), and cyclooctene (0.44 mmol) and carried out in $CDCl_3$ at 20 °C. When TBHP was added last to a mixture of the catalyst and the olefin, the epoxide appears slowly in the first 10 min of the reaction. The rate then increases and becomes linear in the next 20 min, and the buildup continues exponentially.

This kinetic behavior is typical for a catalytic reaction where the catalyst precursor initially reacts with the oxidant to produce the active species in rates slower than or similar to the rate of the reaction of the active species with the substrate. In addition, the reaction rate in the later stages of the reaction becomes slower, indicating that the catalyst is partially deactivated. It has been previously reported that the accumulation of t-BuOH as a byproduct deactivates the catalyst, most likely by adduct formation.[7,9,10,15]

In this catalytic system, **1** reacts with TBHP to form **2** and **3**. One or both of them could be the active species, directly epoxidizing the olefin or acting as catalysts to activate TBHP toward epoxidation. To get further insight on the catalytic cycle, **3** was isolated and its activity tested with different substrates (cyclooctene, $\beta$-methylstyrene, and $\beta$-methoxystyrene).

In the absence of TBHP, both Mo(VI) species are inactive toward the epoxidation of cyclooctene and $\beta$-methoxystyrene at room temperature. However, when excess TBHP is added, the catalytic reaction proceeds. The epoxidation of cyclooctene and $\beta$-methylstyrene leads to the corresponding epoxides only,

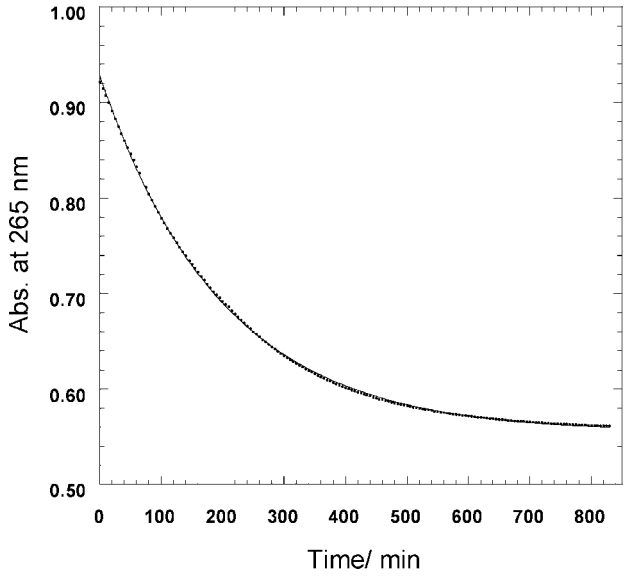


**Figure 5.** Absorbance−time curve at 265 nm for the oxidation of $\beta$-methoxystyrene (0.1 mM) with TBHP (10 mM) catalyzed by **3** (0.4 mM) in $CH_2Cl_2$ at 20 °C.

**Scheme 3. General Reaction Scheme for the Oxidation of 1 by TBHP and the Epoxidation Activity of the Oxidation Products, 2 and 3**

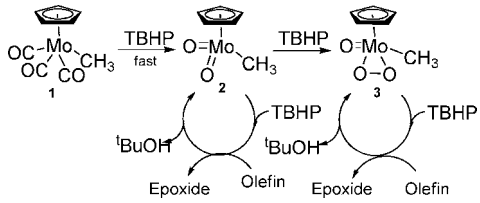


whereas the oxidation of $\beta$-methoxystyrene produces benzaldehyde. Similar behavior was observed for the oxidation of $\beta$-methoxystyrene with Re(VII)-peroxo species as a catalyst. The reaction initially produces the epoxide, which is not stable due to the electron-donating ability of the methoxy group, and undergoes C−C bond cleavage leading to benzaldehyde as the final product.[12e]

A general pathway (Scheme 3) for this catalytic reaction can thus be proposed, involving three Mo species: the carbonyl (**1**), the dioxo (**2**), and the oxo-peroxo (**3**) complexes. Kinetically, it is possible to investigate the proposed pathways by studying each species separately.

**Epoxidations Utilizing $CpMoO(O)_2CH_3$ (3).** Compound **3** was found to catalyze the epoxidation of cyclooctene and styrene with TBHP as oxidizing agent at room temperature. Figure 5 shows the change in the absorbance with time at 265 nm due to the epoxidation of $\beta$-methoxystyrene by the TBHP/**3** system. In the absence of TBHP, the olefin is not oxidized, nor does it react in any form with **3** (when **3** was mixed with cyclooctene or $\beta$-methoxystyrene, no changes were observed by NMR and UV spectroscopy). However, as discussed above, UV experiments show that **3** reacts with TBHP in the absence of olefin. This suggests that the epoxidation of the olefin is carried out by an active intermediate **I**, which is formed by the reaction of **3** with TBHP (Scheme 4).

Although both homolytic and heterolytic activation of peroxides by metal catalysts is possible, activation of TBHP by a homolytic cleavage of the O−O bond (which would generate reactive radicals, such as RO$^\bullet$ or HO$^\bullet$) does not occur due to the reaction insensitivity to oxygen. Also, the olefin reactivity,

**Scheme 4. General Mechanism for the Oxidation of $CpMo(CO)_3CH_3$ (1) and Catalytic Activity of the Resulting Complexes in the Presence of TBHP**

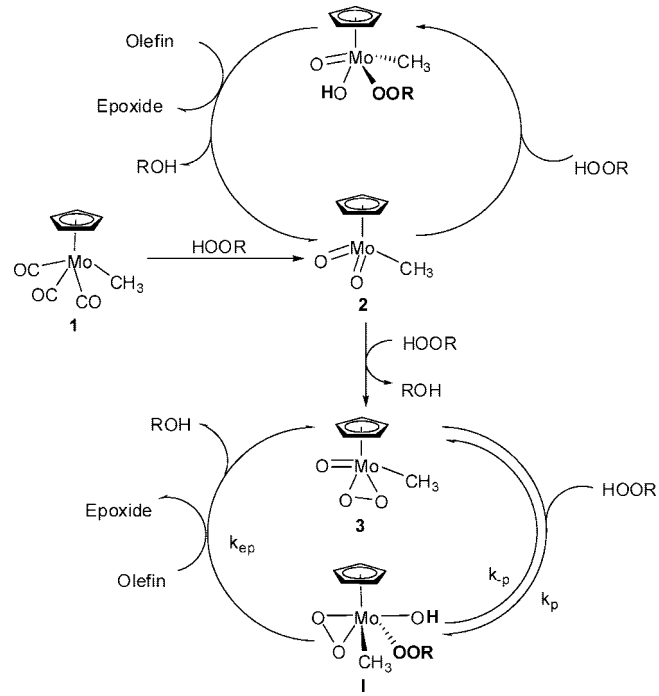


which was found to increase with the olefin nucleophilicity rather than with the radical stability, does not support a radical mechanism. Furthermore, radical mechanisms have not been proposed by the previous studies on epoxidations catalyzed by similar Mo compounds.[6] Therefore, it appears reasonable to assume that the reactive intermediate (**I**), in equilibrium with the catalyst, transfers an O-atom to the olefin to form the epoxide and regenerate the catalyst (Scheme 4).

During the catalytic reaction, the concentration of **I** can be defined by either a steady-state approximation or a pre-equilibrium condition. The epoxidation rate according to Scheme 4 is expressed by eq 3:

$$\text{rate} = \frac{-\text{d[olefin]}}{\text{d}t} = k_{\text{ep}}[\text{olefin}][\mathbf{I}] \tag{3}$$

If the rate equation is derived by means of a steady-state approximation for [**I**] with the mass balance expression, $[\text{Mo}]_\text{T} = [\mathbf{3}] + [\mathbf{I}]$, the rate of the reaction can be written as follows:

$$\text{rate} = \frac{k_{\text{ep}}k_{\text{p}}[\text{olefin}][\text{TBHP}][\text{Mo}]_\text{T}}{k_{-\text{p}}+k_{\text{p}}[\text{TBHP}]+k_{\text{ep}}[\text{olefin}]} \tag{4}$$

The kinetics of the epoxidation of $\beta$-methoxystyrene with TBHP catalyzed by **3** were investigated by following the absorbance change due to the consumption of $\beta$-methoxystyrene and the formation of the product(s) in the region 260−270 nm. Kinetic measurements were carried out with a constant concentration of $\beta$-methoxystyrene of 0.1 mM and a constant [TBHP] of 10 mM. The concentration of **3** was varied in the range 0.1−0.5 mM. Reaction mixtures were prepared in a spectrophotometric cell, the last added reagent being TBHP. The initial rates (i.r.) were calculated from the first 5% of the curves by using eq 5.

$$\text{initial rate} = -(1/b\Delta\varepsilon_\lambda)\Delta\text{Abs}_\text{i}/\Delta t \tag{5}$$

where $b$ is the optical path length, $\Delta\varepsilon_\lambda$ is the total change in the molar absorptivity at $\lambda$, and $\Delta\text{Abs}_\text{i}$ is the initial change in the absorbance.

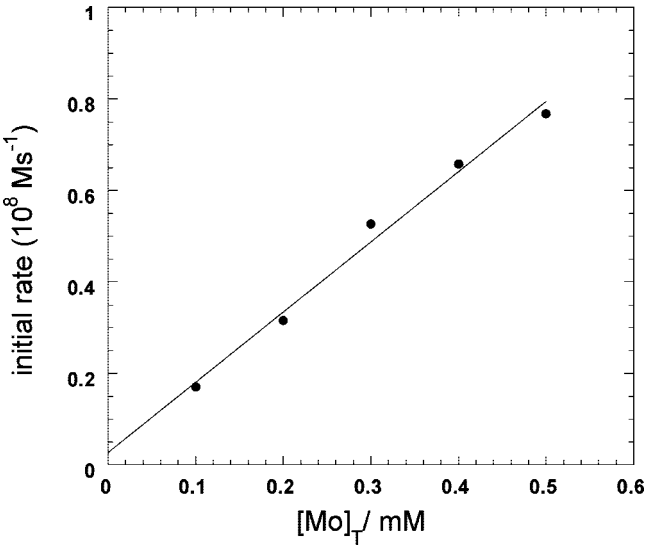


**Figure 6.** Linear variation of the oxidation initial rate of $\beta$-methoxystyrene against $[Mo]_T$ in $CH_2Cl_2$ at 20 °C. [TBHP] = 10 mM, [$\beta$-methoxystyrene] = 0.1 mM.

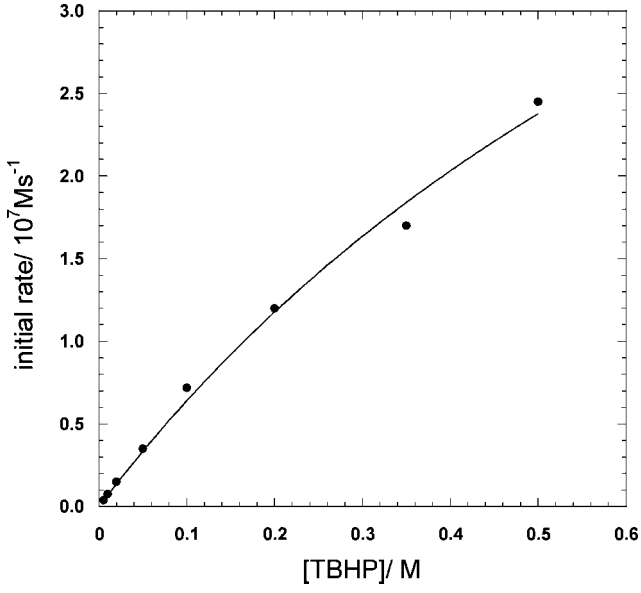


**Figure 7.** Variation of the oxidation initial rate of $\beta$-methoxystyrene (0.1 mM) with TBHP catalyzed by **3** (0.4 mM) in $CH_2Cl_2$ at 20 °C. The data were fitted to eq 4 with the values of $k_p$ (= 0.0047 $M^{-1}$ $s^{-1}$) and $k_{-p}$ (= 0.0032 $s^{-1}$) being held constant and $k_{ep}$ (=18.3 ± 3.8 $M^{-1}$ $s^{-1}$) being varied.

The variation of the initial rate with the catalyst concentration is presented in Figure 6 and shows a linear dependence on $[Mo]_T$, as expected from eq 4. Using the determined values of $k_p$ and $k_{-p}$ (0.0047 $M^{-1}$ $s^{-1}$ and 0.0032 $s^{-1}$, respectively) and the initial concentrations of $\beta$-methoxystyrene and TBHP, the value of $k_{ep}$ (~16 $M^{-1}$ $s^{-1}$) was determined from the slope.

Kinetic measurements were also carried out with a constant $[Mo]_T$ (**3**) of 0.4 mM and a constant concentration of $\beta$-methoxystyrene of 0.1 mM, varying the concentration of TBHP in the range 5−500 mM. A low concentration of $\beta$-methoxystyrene was used to allow direct measurement of the absorbance change, since $\beta$-methoxystyrene has a very strong absorptivity in the UV region ($\varepsilon_{265} \approx 2 \times 10^4$ $M^{-1}$ $cm^{-1}$). A plot of the initial rate against [TBHP] is shown in Figure 7. At low [TBHP] (≤20 mM), the initial rate varies linearly and is first-order with respect to [TBHP]. The order decreases with increasing [TBHP]. This kinetic behavior agrees with the rate law derived on the basis of a steady-state approximation (eq 4). Fitting the data in Figure 7 to eq 4 using the known values of $k_p$ (= 0.0047 $M^{-1}$ $s^{-1}$) and $k_{-p}$ (= 0.0032 $s^{-1}$) leads to the epoxidation rate constant ($k_{ep}$ = 18.3 ± 3.8 $M^{-1}$ $s^{-1}$). This value of $k_{ep}$ is close to the value estimated above from varying the concentration of the catalyst.

The reactions of *trans*-$\beta$-methylstyrene (UV method) and cyclooctene (NMR method) were studied similarly, and the values of $k_{ep}$ for their epoxidation with TBHP catalyzed by **3** are 0.5 and 1.3 $M^{-1}$ $s^{-1}$, respectively. These results show that the epoxidation rate constant ($k_{ep}$) increases with the olefin nucleophilicity:

$$\beta\text{-methoxystyrene} \gg \text{cyclooctene} > \textit{trans}\text{-}\beta\text{-methylstyrene}$$

$\beta$-methoxystyrene is the most nucleophilic olefin among the examined substrates (due to the presence of an $OCH_3$ group), and it is ca. 15 times more reactive than cyclooctene.[12]

Additionally, the epoxidation reaction is stereoselective. When *trans*-$\beta$-methylstyrene is oxidized only the trans epoxide is obtained. Epoxidations that occur by an external attack of the nucleophilic olefin onto the electrophilic oxygen of the M-alkylperoxo (or M-peroxo) group by a concerted O-transfer step are usually stereoselective, and coordination of the olefin to the metal center prior to the oxygen transfer step is less likely to happen.[10,16]

**Epoxidation Catalyzed by $CpMoO_2CH_3$ (2).** The profile of the reaction between **1** (0.05 mmol), cyclooctene (0.44 mmol), and TBHP (0.6 mmol) in $CDCl_3$ at 20 °C (Figure 4) indicates the presence of at least two catalytic systems formed from the initial Mo(II) precursor. Each catalyst activates TBHP (through an active intermediate) for the epoxidation of an olefin (as shown in Scheme 3). It was not possible to study the catalytic activity of **2** separately, because in addition to the epoxidation reaction, **2** also reacts with TBHP to form **3**, which also catalyzes the epoxidation of olefin as shown above. However, the values of the rate constants for the reactions of **1** with TBHP to yield **2** and **3** were determined in the absence of the olefin under the same conditions, and the rate constants for the epoxidation of cyclooctene by the TBHP/**3** catalytic system ($k_p$, $k_{-p}$, and $k_{ep}$ in Scheme 4) were determined separately. Therefore, it is possible to estimate the relative rates of the epoxidation reactions by **2** from reactions initially started with the precursor **1** (see Appendix III in the Supporting Information). An initial rate method with the olefin existing in much higher concentration than the catalyst and TBHP was used. The initial rates were calculated from the initial 2−5% conversion of the olefin. Under these conditions, **3** is not involved, and the rate constant for the epoxidation of an olefin by **2**/TBHP was estimated. For cyclooctene, the epoxidation rate constant for reactions catalyzed by compound **2** are 3−5 times higher than those catalyzed by compound **3** under the same conditions, which might originate from the slighty different structure of the intermediates. This shows that **2** is more active than **3**. However, when TBHP is present in large excess over the olefin and the catalyst formation of **3** from **2** occurs at the beginning of the catalytic reaction, most of the epoxidation is carried out by the active species formed from **3** rather than that from **2**.

## 3. Conclusion

Based on detailed kinetic studies and experimental evidence, the mechanism shown in Scheme 4 has been proposed for the catalytic olefin epoxidation promoted by the precursor $CpMo(CO)_3CH_3$ (**1**). In the presence of excess alkyl hydroperoxide (TBHP), $CpMo(O)_2CH_3$ (**2**) and $CpMo(O)(O_2)CH_3$ (**3**)

are formed. Whereas the isolated compound **3** is inactive for stoichiometric epoxidation of cyclooctene and styrenes, epoxidation with **3** does proceed in the presence of TBHP under formation of a reactive species **I**. The kinetic results of the variation of the reaction rate with the alkyl hydroperoxide are consistent with the formation of a $\sigma$-alkylperoxo intermediate species, as has been postulated for other Mo(VI)-based catalyst systems.[12] In the presence of excess olefin, the catalytic system is stable and the major pathway is the catalytic epoxidation reaction. As far as it can be concluded from the published literature, $CpMo(CO)_3CH_3$ differs in several aspects from the previously examined $CpMo(CO)_3Cl$ with respect to its reaction behavior and applicability as catalyst. Work is currently undertaken in our laboratories to examine the apparently different catalytic behavior of the Cl derivative in more detail.

## 4. Experimental Section

**4.1. Material and Methods.** All preparations were carried out under an oxygen- and water-free argon atmosphere using standard Schlenk techniques. All solvents were derived from a MBraun solvent purification system. Cyclooctene and $\beta$-methoxystyrene (Aldrich) were used as received without further purifications. TBHP (Aldrich, 5.0−6.0 M solution in decane) was used after drying over molecular sieves to remove the residual water (<4% when received).

IR spectra were measured with a JASCO FT-IR-460 Plus spectrometer using KBr pellets. NMR spectra were measured applying a JEOL 400 and 400 MHz Bruker Avance DPX-400 spectrometer. The UV spectra were measured on a JASCO UV−vis V-550 spectrophotometer.

**4.2. Synthesis of $CpMo(O_2)OCH_3$.** $CpMo(CO)_3CH_3$ (1 mmol, 260 mg) was mixed with 10 equiv of TBHP (10 mmol) in 40 mL of dichloromethane at room temperature. The oxidation continued for 3 h, and then $MnO_2$ was added to quench the reaction. After another 1 h stirring, the solution was filtrated to removed $MnO_2$ and any solid residue. Then the solvent was evaporated under vacuum at 0 °C. The pale yellow solid was washed three times with hexane (3 × 5 mL) and dried under vacuum. Yield: ∼140 mg (63%). Elemental analysis (C, 32.06; H, 3.76) is in agreement with the calculated values for $C_6H_8O_3Mo$ (224.06): C, 32.17; H, 3.60. The spectral data of the pure compound are in agreement with those reported for the Mo-oxoperoxo compound, $CpMo(O)(O_2)CH_3$, prepared previously by the method of Legzdins.[15] IR (KBr, $\nu$ cm$^{-1}$): 3102s (Cp), 3064w, 2987w, 2943w, 2895w, 1633bw, 1454w, 1420m, 1169m, 1067m, 1029m, 1002m, 951vs ($\nu_{Mo=O}$), 931s, 877vs ($\nu_{O-O}$), 849s, 831s, 774w, 748w, 575s, 565s ($\nu_{Mo-O}$). $^1$H NMR ($CDCl_3$, 400 MHz, rt, $\delta$ ppm): 6.29 (5H, s, Cp), 2.12 (3H, s, $CH_3$). $^{13}$C NMR ($C_6D_6$, 100.28 MHz, rt, $\delta$ ppm): 109.3 (Cp), 24.7 ($CH_3$). $^{95}$Mo NMR ($C_6D_6$, 26.07 MHz, rt, $\delta$ ppm): −609 ppm. $^{17}$O NMR ($CDCl_3$, 54.26 MHz, rt, $\delta$ ppm): 869 (oxo), 359, 336 (peroxo).

**4.3. Kinetic Studies.** Kinetic data were collected by using $^1$H NMR and UV methods. The epoxidation of cyclooctene was monitored by NMR, and the epoxidation of $\beta$-methoxystyrene was followed by UV spectrophotometric technique. In every case the temperature was controlled at 20 °C. (a) The reactions studied by $^1$H NMR were carried out in $CDCl_3$ in a total volume of 0.5−1.0 mL. The relative amounts of TBHP, the catalyst, and cyclooctene were chosen with concern for the requirements of the kinetic analysis, which was carried out by first-order or initial rate kinetics. The $^1$H NMR spectra were recorded at 2−20 min increments over the 2−5 h reaction time. Under pseudo-first-order conditions, the changes in the intensity ($I$) of the cyclooctene signal(s) and/or the cyclooctene oxide with time were fit to a single-exponential decay: $I_t = I_\infty + (I_o - I_\infty) \exp(-k_\Psi t)$. (b) In the spectrophotometric (UV) method, the reaction mixtures were prepared in the reaction cuvette (optical path = 1.0 cm, $V_T$ = 3.0 mL) with the last component added being TBHP or the olefin. Some experiments were carried out in cuvettes with short optical paths (0.1−0.2 cm) to allow direct measurement of the absorbance changes during the reaction when the catalyst or $\beta$-methoxystyrene were varied, because both have high molar absorptivities and contribute a large absorbance background at the wavelengths used. The data were obtained by following the loss of the $\beta$-methoxystyrene (or *trans*-$\beta$-methylstyrene) absorption in the range 260−270 nm. Initial rate and pseudo-first-order conditions were applied in different protocols. In the latter case, the pseudo-first-order rate constants were evaluated by nonlinear least-squares fitting of the absorbance−time curves to a single-exponential equation, $A_t = A_\infty + (A_o - A_\infty) \exp(-k_\Psi t)$.

**Acknowledgment.** A.M.A. thanks the Alexander von Humboldt Foundation for a Georg Forster Fellowship and Jordan University of Science and Technology for a sabbatical vacation. J.Z. thanks the Hochschul- and Wissenschaftsprogramm (HWP-II): Fachprogramm Chancengleichheit für Frauen in Forschung and Lehre for a postdoctoral grant. E.H. thanks Stephan D. Hoffmann for experimental assistance. M.J.C. thanks FCT and FEDER for financial support (POCI/QUI/58925/2004).

**Supporting Information Available:** X-ray data, complete derivations of eqs 1 and 4, and an estimation of the relative values for the rate constant of the catalysis with compound **2**. This material is available free of charge via the Internet at http://pubs.acs.org.

OM8009206